

$$M \begin{pmatrix} A & B \\ C & D \end{pmatrix} M^{-1} = \begin{pmatrix} e^{iK\Lambda} & 0 \\ 0 & e^{-iK\Lambda} \end{pmatrix}, \quad (\text{B9})$$

then the  $N$ th power of the  $ABCD$  matrix is immediately given by

$$\begin{pmatrix} A & B \\ C & D \end{pmatrix}^N = M^{-1} \begin{pmatrix} e^{iNK\Lambda} & 0 \\ 0 & e^{-iNK\Lambda} \end{pmatrix} M. \quad (\text{B10})$$

The matrix  $M$  which transforms the  $ABCD$  matrix into a diagonal matrix can be constructed from the eigenvectors (B6) of the  $ABCD$  matrix.  $M$  and its inverse  $M^{-1}$  are given by

$$M^{-1} = \frac{1}{(\alpha_+\beta_- - \alpha_-\beta_+)^{1/2}} \begin{pmatrix} \alpha_+ & \alpha_- \\ \beta_+ & \beta_- \end{pmatrix}, \quad (\text{B11})$$

$$M = \frac{1}{(\alpha_+\beta_- - \alpha_-\beta_+)^{1/2}} \begin{pmatrix} \beta_- & -\alpha_- \\ -\beta_+ & \alpha_+ \end{pmatrix}. \quad (\text{B12})$$

The two columns in (B11) are simply the eigenvectors of the  $ABCD$  matrix. It can be easily seen by simple matrix multiplication that (B9) is true as long as  $M$  and  $M^{-1}$  are given by (B12) and (B11), respectively. The Chebyshev identity (B1) follows directly from (B10) by carrying out the matrix multiplication:

$$\begin{aligned} \begin{pmatrix} A & B \\ C & D \end{pmatrix}^N &= \frac{1}{\alpha_+\beta_- - \alpha_-\beta_+} \begin{pmatrix} \alpha_+ & \alpha_- \\ \beta_+ & \beta_- \end{pmatrix} \\ &\quad \times \begin{pmatrix} e^{iNK\Lambda} & 0 \\ 0 & e^{-iNK\Lambda} \end{pmatrix} \begin{pmatrix} \beta_- & -\alpha_- \\ -\beta_+ & \alpha_+ \end{pmatrix} \\ &= \begin{pmatrix} \frac{A \sin NK\Lambda - \sin(N-1)K\Lambda}{\sin K\Lambda} & \frac{B \sin NK\Lambda}{\sin K\Lambda} \\ \frac{C \sin NK\Lambda}{\sin K\Lambda} & \frac{D \sin NK\Lambda - \sin(N-1)K\Lambda}{\sin K\Lambda} \end{pmatrix}. \end{aligned} \quad (\text{B14})$$

The last step is left to the reader.

## Electromagnetic propagation in periodic stratified media. II. Birefringence, phase matching, and x-ray lasers\*

Amnon Yariv and Pochi Yeh

California Institute of Technology, Pasadena, California 91125

(Received 8 November 1976)

The theory of electromagnetic Bloch waves in periodic stratified media is applied to the problems of birefringence and group velocity in these media. The relevance of periodic media to phase matching in nonlinear mixing experiments and to laser action in the x-ray region is discussed.

### I. PHASE VELOCITY AND GROUP VELOCITY

We have derived in paper I<sup>1</sup> some of the important characteristics of Bloch waves propagating in a periodic stratified medium. An exact expression for the dis-

\*Research supported by the Office of Naval Research and the NSF.

<sup>1</sup>F. Abeles, *Ann. Phys. (Paris)* 5, 596 (1950); 5, 706 (1950).

<sup>2</sup>A. Ashkin and A. Yariv, *Bell Labs. Tech. Memo MM-61-124-46* (13 November 1961) (unpublished).

<sup>3</sup>N. Bloembergen and A. J. Sievers, *Appl. Phys. Lett.* 17, 483 (1970).

<sup>4</sup>C. L. Tang and P. P. Bey, *IEEE J. Quantum Electron.* QE-9, 9 (1973).

<sup>5</sup>S. M. Rytov, *Zh. Eksp. Teor. Fiz.* 29, 605 (1955) [*Sov. Phys. -JETP* 2, 466 (1956)].

<sup>6</sup>J. P. van der Ziel, M. Illegems, and R. M. Mikulyak, *Appl. Phys. Lett.* 28, 735 (1976).

<sup>7</sup>A. Y. Cho and J. R. Arthur, *Progress in Solid State Chemistry*, Vol. 10 (Pergamon, New York, 1975), Part 3, pp. 157-159.

<sup>8</sup>A. Yariv, *Appl. Phys. Lett.* 25, 105 (1974).

<sup>9</sup>F. Bloch, *Z. Phys.* 52, 555 (1928).

<sup>10</sup>K. Aiki, M. Nakamura, J. Umeda, A. Yariv, A. Katzir, and H. W. Yen, *Appl. Phys. Lett.* 27, 145 (1975).

<sup>11</sup>H. C. Casey, Jr., S. Somekh, and M. Illegems, *Appl. Phys. Lett.* 27, 142 (1975).

<sup>12</sup>F. K. Reinhart, R. A. Logan, and C. V. Shank, *Appl. Phys. Lett.* 27, 45 (1975).

<sup>13</sup>A. Yariv, *IEEE J. Quant. Electron.* QE-9, 919 (1973).

<sup>14</sup>M. Born and E. Wolf, *Principles of Optics* (Macmillan, New York, 1964), p. 67.

<sup>15</sup>H. Yajima, *Proceedings of the Symposium on Optical and Acoustical Micro-Electronics*, New York, April 1974 (unpublished).

<sup>16</sup>L. B. Stotts, *Opt. Commun.* 17, 133 (1976).

<sup>17</sup>S. Somekh, E. Garmire, A. Yariv, H. Garvin, and R. Hunsperger, *Appl. Phys. Lett.* 22, 46 (1973).

<sup>18</sup>A. B. Buckman, *J. Opt. Soc. Am.* 66, 30 (1976).

<sup>19</sup>E. A. Ash, "Grating Surface Waveguides," presented at International Microwave Symposium, Newport Beach, Calif., May 1970 (unpublished).

<sup>20</sup>A. Yariv, *Quantum Electronics* (Wiley, New York, 1975).

<sup>21</sup>P. K. Tien, *Appl. Opt.* 10, 2395 (1971).

<sup>22</sup>D. Kossel, "Analogies between Thin-Film Optics and Electron-Band Theory of Solids," *J. Opt. Soc. Am.* 56, 1434 (1966).

<sup>23</sup>J. A. Arnaud and A. A. M. Saleh, *Appl. Opt.* 13, 2343 (1974).

<sup>24</sup>W. Shockley, *Phys. Rev.* 56, 317 (1939).

<sup>25</sup>J. P. van der Ziel and M. Illegems, *Appl. Phys. Lett.* 28, 437 (1976).

persion relation between  $K$ ,  $\beta$ , and  $\omega$  was derived. This dispersion relation can be represented by contours of constant frequency in the  $\beta$ - $K$  plane as in Fig. 1.

It can be seen that these contours are more or less

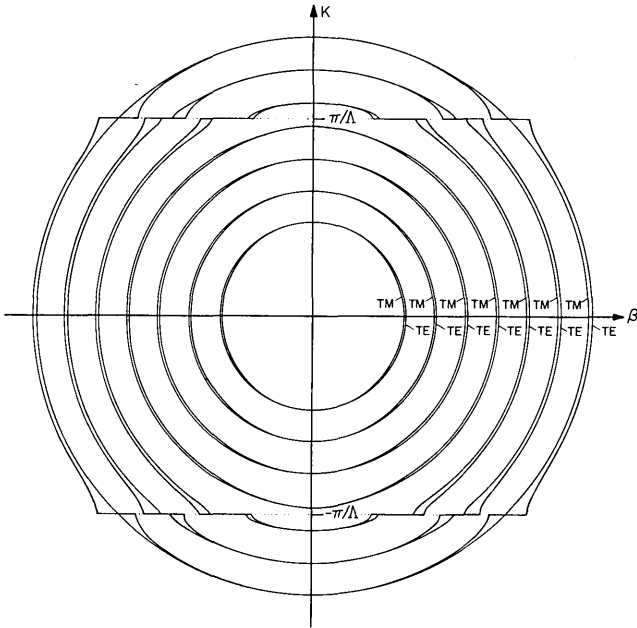


FIG. 1. Contours of constant frequency in  $\beta$ - $K$  plane.

circular with only a slight ellipticity. The origin corresponds to the contour of zero frequency. In the long-wavelength regime ( $\lambda \gg \Lambda$ ), these are similar to the dispersion curves of electromagnetic waves in a negative uniaxial crystal. The birefringence property of a periodic stratified medium will be discussed further in Sec. II. These contours become distorted and modified at shorter wavelengths and near the boundaries of the Brillouin zone ( $K\Lambda = l\pi$ ) where the wavelength is comparable with the dimension of a unit cell and the electromagnetic waves interact strongly with the periodic medium.

The concepts of phase and group velocities in periodic layered media are subtle and require careful examination. Let us start by reviewing some of the relevant results which were derived in paper I.

The electromagnetic Bloch wave is given by

$$\mathbf{E}(x, z, t) = \mathbf{E}_K(x) e^{iKx} e^{i\beta z} e^{-i\omega t}, \quad (1)$$

where  $\mathbf{E}_K(x)$  is a periodic function of  $x$  with period  $\Lambda$  and is given by Eq. (28) in paper I. The dispersion relation between  $K$ ,  $\beta$ , and  $\omega$  is given by

$$\cos K\Lambda = \frac{1}{2}(A + D) = \cos k_{1x} a \cos k_{2x} b - \Delta \sin k_{1x} a \sin k_{2x} b, \quad (2)$$

where  $A$  and  $D$  are given, respectively, by Eqs. (10), (13), (15), and (18) of paper I and

$$\Delta = \begin{cases} \frac{1}{2}(k_{2x}/k_{1x} + k_{1x}/k_{2x}), & \text{TE waves,} \\ \frac{1}{2}(n_2^2 k_{1x}/n_1^2 k_{2x} + n_1^2 k_{2x}/n_2^2 k_{1x}), & \text{TM waves;} \end{cases} \quad (3)$$

$$k_{1x} = \{[(\omega/c)n_1]^2 - \beta^2\}^{1/2}, \quad (4)$$

$$k_{2x} = \{[(\omega/c)n_2]^2 - \beta^2\}^{1/2}. \quad (5)$$

It is important to note that the Bloch wave number  $K$  given by (2) is not uniquely defined to the extent that any integer multiple of  $2\pi/\Lambda$  can be added to it. The reduced Brillouin zone scheme commonly used in solid-state physics is no longer useful as far as the phase

velocity of an electromagnetic Bloch wave is concerned. If  $\mathbf{E}_K(x)$  is expanded in a Fourier series

$$\mathbf{E}_K(x) = \sum_n \mathbf{e}_K^{(n)} e^{in(2\pi/\Lambda)x}, \quad (6)$$

The Bloch wave (1) can be written as a linear superposition of an infinite number of partial plane waves which are the so-called "space harmonics." From (1) and (6) we have

$$\mathbf{E}(x, z, t) = \sum_n \mathbf{e}_K^{(n)} e^{i[K+n(2\pi/\Lambda)]x} e^{i\beta z} e^{-i\omega t}, \quad (7)$$

where  $\mathbf{e}_K^{(n)}$  are constants. Thus the multivalued nature of the Bloch wave number embodies the existence of the whole set of space harmonics. If the periodicity is removed, i. e.,  $n_1 = n_2 = n$  then the Bloch mode should become an ordinary plane wave and  $K$  should be equal to  $k_x = (\omega/c)n \cos \theta$ . Equation (2) in this case reads

$$\cos K\Lambda = \cos[k_x(a+b)] = \cos k_x \Lambda,$$

so that when  $n_1 - n_2 \ll n_1$ , the principal value of  $K$  can be chosen as that nearest to  $k_{1x}$  or  $k_{2x}$ . We can ensure that  $K$  satisfies the above condition by choosing it in such a way that

$$|\mathbf{e}_K^{(0)}| \geq |\mathbf{e}_K^{(n)}| \quad (8)$$

for all  $n$ , or equivalently by choosing  $K$  such that the integral

$$\frac{1}{\Lambda} \int_0^\Lambda \mathbf{E}_K(x) dx \equiv \langle \mathbf{E}_K \rangle \quad (9)$$

has a maximum value.

Having a proper choice of the Bloch wave number  $K$  we are now in a position to define the phase velocity of a Bloch wave. It is defined as

$$V_p = \omega / (K^2 + \beta^2)^{1/2}. \quad (10)$$

The phase velocity defined above is, strictly speaking, the phase velocity of the fundamental ( $n=0$ ) space harmonic which is a plane wave of the form

$$\mathbf{E}(x, z, t) = \langle \mathbf{E}_K \rangle e^{iKx} e^{i\beta z} e^{-i\omega t}. \quad (11)$$

In the long-wavelength regime where the whole structure behaves as if it were homogeneous, the fundamental space harmonic is the dominant part of the Bloch wave and can be taken alone as a very good approximation of the whole wave.

The group velocity for a Bloch wave packet is given by

$$\mathbf{V}_g = \left( \frac{\partial \omega}{\partial K} \right)_\beta \hat{a}_x + \left( \frac{\partial \omega}{\partial \beta} \right)_K \hat{a}_z. \quad (12)$$

In a homogeneous medium the group velocity represents the velocity of energy flow of a quasimonochromatic wave and is thus parallel to the Poynting vector which is a constant vector in a homogeneous lossless medium. The Poynting vector of a Bloch wave given by (1) is a periodic function of  $x$ . The group velocity (12) of the same wave, however, is a constant vector. The discrepancy is due to the fact that in a periodic medium the power flow is a periodic function of the space coordinates. We will show, however, that the averaged

velocity of energy flow defined as

$$\mathbf{V}_e = \left( \frac{1}{\Lambda} \int_0^\Lambda (\text{Poynting vector}) dx \right) \times \left( \frac{1}{\Lambda} \int_0^\Lambda (\text{energy density}) dx \right)^{-1} \quad (13)$$

is exactly equal to the group velocity as given by (12) (see Appendix A). This endows the concept of group velocity as defined by (12) with a rigorous meaning. It is an extremely useful concept since it now makes it possible to consider the propagation of confined finite aperture beams in a layered medium. The space averaged Poynting vector and energy density are particularly useful in the long-wavelength regime where the medium can be considered as a quasihomogeneous and anisotropic medium.

## II. BIREFRINGENCE OF PERIODIC STRATIFIED MEDIA

In this section we review the birefringence which results from the medium periodicity. We start by reviewing in the context of our present discussion the birefringent behavior of bulk anisotropic media.

The index of refraction of light propagating in an anisotropic medium depends on its state of polarization. Given a direction of propagation in the medium there are, in general, two eigenpolarizations with two respective eigenphase velocities. The directions of eigenpolarization and their corresponding indices of refraction for a plane wave of the following form:

$$\mathbf{E}(\mathbf{r}, t) = \mathbf{E} e^{i[(\omega/c)n\mathbf{s} \cdot \mathbf{r} - \omega t]} \quad (14)$$

are given by the following well-known formulas<sup>2</sup>:

$$\frac{s_x^2}{n^2 - \epsilon_x/\epsilon_0} + \frac{s_y^2}{n^2 - \epsilon_y/\epsilon_0} + \frac{s_z^2}{n^2 - \epsilon_z/\epsilon_0} = \frac{1}{n^2}, \quad (15)$$

$$E_i = \frac{n^2 s_i (\mathbf{s} \cdot \mathbf{E})}{n^2 - \epsilon_i/\epsilon_0}, \quad i = x, y, z, \quad (16)$$

where  $\epsilon_x, \epsilon_y, \epsilon_z$  are the principal dielectric constants and  $\mathbf{s}$  is a unit vector along the direction of polarization.

Equation (15) (also known as Fresnel's equation of wave normals) can be solved for the eigenindices of refraction, while Eq. (16) gives the directions of polarization.

It is important to notice that Eq. (15) is in fact the dispersion relation between  $\omega$  and  $\mathbf{k}$ . If we define  $\mathbf{k}$  as  $(\omega/c)n\mathbf{s}$  for the plane wave given by (14), then Eq. (15) can be written

$$\frac{k_x^2}{k^2 - (\omega^2/c^2)\epsilon_x/\epsilon_0} + \frac{k_y^2}{k^2 - (\omega^2/c^2)\epsilon_y/\epsilon_0} + \frac{k_z^2}{k^2 - (\omega^2/c^2)\epsilon_z/\epsilon_0} = 1, \quad (17)$$

where

$$k^2 = k_x^2 + k_y^2 + k_z^2. \quad (18)$$

Equation (17) describes a surface of two shells in  $\mathbf{k}$  space known as the normal surface. The two shells of the normal surface have only four points in common. The two lines which go through the origin and these

points are known as the optical axes. Given a direction of propagation, there are in general two  $k$  values which are the intersections of the direction of propagation and the normal surface. These two  $k$  values correspond to two different phase velocities  $\omega/k$  of the waves propagating along the chosen direction.

Equation (17) can also be derived directly from the wave equation

$$\nabla \times (\nabla \times \mathbf{E}) + \mu \bar{\epsilon} \frac{\partial^2}{\partial t^2} \mathbf{E} = 0. \quad (19)$$

Substitution for  $\mathbf{E}$  from (14) gives, if we also recall  $\mathbf{k} = (\omega/c)n\mathbf{s}$ :

$$\mathbf{k} \times (\mathbf{k} \times \mathbf{E}) = \mu \bar{\epsilon} \frac{\partial^2}{\partial t^2} \mathbf{E}, \quad (20)$$

or equivalently

$$\begin{pmatrix} \omega^2 \mu \epsilon_x - k_y^2 - k_z^2 & k_x k_y & k_x k_z \\ k_y k_x & \omega^2 \mu \epsilon_y - k_x^2 - k_z^2 & k_y k_z \\ k_z k_x & k_z k_y & \omega^2 \mu \epsilon_z - k_x^2 - k_y^2 \end{pmatrix} \times \begin{pmatrix} E_x \\ E_y \\ E_z \end{pmatrix} = 0. \quad (21)$$

In order to have a nontrivial plane wave solution, the determinant of the matrix in (21) must vanish. This gives us Eq. (22), which is equivalent to the dispersion relation (17), if we recall  $c^2 = 1/\mu\epsilon_0$ :

$$\det \begin{vmatrix} \omega^2 \mu \epsilon_x - k_y^2 - k_z^2 & k_x k_y & k_x k_z \\ k_y k_x & \omega^2 \mu \epsilon_y - k_x^2 - k_z^2 & k_y k_z \\ k_z k_x & k_z k_y & \omega^2 \mu \epsilon_z - k_x^2 - k_y^2 \end{vmatrix} = 0. \quad (22)$$

Of particular interest is the uniaxial crystal with a normal surface consisting of a sphere and an ellipsoid of revolution. If we set  $\epsilon_y = \epsilon_z$  in Eq. (17), the equation breaks into two factors, giving

$$\frac{k_x^2}{n_o^2} + \frac{k_y^2 + k_z^2}{n_e^2} = \frac{\omega^2}{c^2}, \quad (23)$$

$$\frac{k_x^2}{n_o^2} + \frac{k_y^2 + k_z^2}{n_o^2} = \frac{\omega^2}{c^2}, \quad (24)$$

where

$$n_o^2 = \epsilon_x/\epsilon_0, \quad n_e^2 = \epsilon_y/\epsilon_0. \quad (25)$$

The section of the normal surface by the coordinate plane  $k_y = 0$  is a circle and an ellipse (see Fig. 2). The line joining the origin and the osculating points of the circle and the ellipse is the optical axis.

It can easily be shown that the vectors  $\mathbf{E}$  and  $\mathbf{H}$  always lie in the tangent plane of the normal surface. As a result the Poynting vector  $\mathbf{S}$  defined by

$$\mathbf{S} = \mathbf{E} \times \mathbf{H} \quad (26)$$

is always parallel to the group velocity which is given by

$$\mathbf{V}_g = \nabla_{\mathbf{k}} \omega(\mathbf{k}). \quad (27)$$

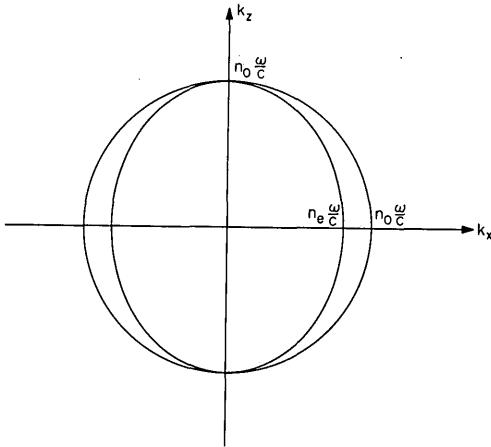


FIG. 2. Section of normal surface in  $k_x$ - $k_z$  plane.

To prove that  $\mathbf{S}$  and  $\mathbf{V}_g$  are parallel, we start from Eq. (20) and replacing  $\partial/\partial t$  by  $-i\omega$  rewrite it

$$\mathbf{k} \times (\mathbf{k} \times \mathbf{E}) + \omega^2 \mu \bar{\epsilon} \mathbf{E} = 0. \quad (28)$$

Suppose now that  $\mathbf{k}$  is changed by a small amount  $\delta\mathbf{k}$  while  $\omega$  is kept constant. If  $\delta\mathbf{E}$  is the corresponding change in  $\mathbf{E}$ , we have, according to (28),

$$\delta\mathbf{k}(\mathbf{k} \cdot \mathbf{E}) + \mathbf{k}(\delta\mathbf{k} \cdot \mathbf{E}) + \mathbf{k}(\mathbf{k} \cdot \delta\mathbf{E}) - \delta\mathbf{E}(\mathbf{k} \cdot \mathbf{k}) - 2\mathbf{E}(\mathbf{k} \cdot \delta\mathbf{k}) + \omega^2 \mu \bar{\epsilon} \delta\mathbf{E} = 0 \quad (29)$$

If we multiply both sides of this equation by  $\mathbf{E}$ , we obtain, using  $\epsilon_{ij} = \epsilon_{ji}$ ,

$$2\delta\mathbf{k} \cdot [\mathbf{k}(\mathbf{E} \cdot \mathbf{E}) - \mathbf{E}(\mathbf{k} \cdot \mathbf{E})] + \delta\mathbf{E} \cdot [\mathbf{k}(\mathbf{E} \cdot \mathbf{k}) - \mathbf{E}(\mathbf{k} \cdot \mathbf{k}) + \omega^2 \mu \bar{\epsilon} \mathbf{E}] = 0. \quad (30)$$

The second term vanishes according to (28) and the first term can be written  $2\delta\mathbf{k} \cdot [\mathbf{E} \times (\mathbf{k} \times \mathbf{E})]$ . Hence, we have, using  $\mathbf{H} = (1/\omega\mu)\mathbf{k} \times \mathbf{E}$ ,

$$\delta\mathbf{k} \cdot (\mathbf{E} \times \mathbf{H}) = 0, \quad (31)$$

i. e.,  $\mathbf{E} \times \mathbf{H}$  is perpendicular to  $\delta\mathbf{k}$  which is an arbitrary infinitesimal vector in the tangent plane of the normal surface. The group velocity  $\mathbf{V}_g$  defined by (27) is also perpendicular to the normal surface, thus proving our statement.

Let us now consider the propagation of electromagnetic waves in a medium consisting of infinitely alternating layers of two different homogeneous and isotropic substances. Although each individual layer is isotropic, the whole structure behaves as an anisotropic medium. TE waves and TM waves are found to propagate with different effective phase velocities and the periodic medium is birefringent. This phenomenon is well known in an anisotropic homogeneous crystal and is used in the electrooptic modulation of light and in a variety of polarizing applications.

The electromagnetic properties of a periodic laminated structure have been studied by Rytov,<sup>3</sup> who limited his treatment to cases in which the direction of propagation is either parallel or normal to the layers. In the present analysis we use the Bloch wave formalism of Paper I to obtain the exact birefringence behavior of

a periodic medium for waves propagating in an arbitrary direction.

It was shown above that the only dynamical variables needed to describe a monochromatic plane wave propagating in a periodic stratified medium are  $\omega$ ,  $\beta$ , and  $K$ . The generalized wave vector is defined

$$\boldsymbol{\kappa} = \hat{a}_x K + \hat{a}_z \beta. \quad (32)$$

The dispersion relation between  $\omega$  and  $\boldsymbol{\kappa}$  is given by Eq. (2).

If the period  $\Lambda$  is sufficiently small compared to the wavelength, then the whole structure behaves as if it were homogeneous and uniaxially anisotropic. The wave given by (1) thus behaves as if it were a plane wave of the form given by (11).

In Fig. 1 the contours of constant  $\omega$  are plotted in the  $K$ - $\beta$  plane. These are sections of the normal surfaces with the  $K$ - $\beta$  plane for various frequencies. It is evident from inspection that at the long-wavelength limit ( $\lambda \gg \Lambda$ ) the dispersion of a layered medium is qualitatively similar to that of a negative uniaxial crystal.

To demonstrate this analogy we take the limit of  $k_{1x}a \ll 1$ ,  $k_{2x}b \ll 1$ , and  $K\Lambda \ll 1$  and expand all the transcendental functions in (2). After neglecting higher-order terms, we obtain

$$K^2/n_o^2 + \beta^2/n_o^2 = \omega^2/c^2, \quad \text{TE}, \quad (33)$$

$$K^2/n_o^2 + \beta^2/n_e^2 = \omega^2/c^2, \quad \text{TM}, \quad (34)$$

with

$$n_o^2 = (a/\Lambda)n_1^2 + (b/\Lambda)n_2^2, \quad (35)$$

$$1/n_e^2 = (a/\Lambda) \cdot (1/n_1^2) + (b/\Lambda) \cdot (1/n_2^2). \quad (36)$$

Equations (27) and (28) represent the two shells of the normal surface in the  $K$ - $\beta$  plane. One surface (33) applies to a TE wave and is a sphere while the TM normal surface (34) is an ellipsoid of revolution. TE waves thus are formally analogous to the so-called ordinary waves in a uniaxial crystal, while TM waves are the extraordinary waves. The normal surface becomes more complicated at higher frequencies. It consists of two oval surfaces osculating each other at the intersections with the  $K$  axis as long as the frequency is below the first forbidden gap. For frequencies higher than the forbidden gap, the oval surfaces break into several sections. The break points occur at

$$K = m(\pi/\Lambda), \quad m = \text{integer}, \quad (37)$$

which is the Bragg condition for the quasi-plane-wave (11).

### III. DOUBLE REFRACTION AT A BOUNDARY

Consider a plane wave incident on the surface of a semi-infinite periodic stratified medium. If the incident wave is a mixture of TE and TM waves, double refraction takes place. This can be easily seen from the normal surface in the  $\beta$ - $K$  plane. A very important kinematic property of refraction at a plane interface

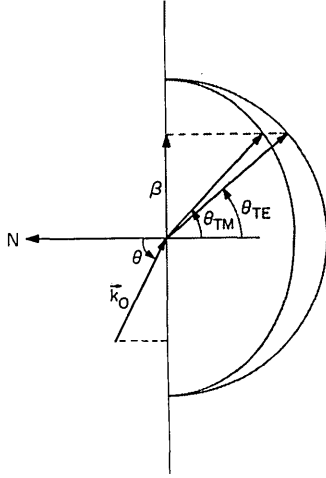


FIG. 3. Double refraction at the boundary of a periodic stratified medium.

between two dielectric media is the fact that  $\beta$ , the tangential component of the wave vectors, must be equal for both the incident and refracted waves. Given a  $\beta$  value, the two shells of the normal surface in general yields two  $K$  values, thus giving rise to two refracted waves as shown in Fig. 3. The two refracted waves are in general both extraordinary waves in the sense that their phase velocities, i. e., effective indices, depend on  $\beta$ .

However, at the long-wavelength regime where  $\lambda \gg \Lambda$ , TE waves become ordinary waves while TM waves remain extraordinary. If the wave vector of the incident wave is denoted by  $\mathbf{k}_0$ , and  $\theta$  is the angle of incidence, the projection of the wave vector along the boundary plane is given by

$$\beta = k_0 \sin \theta. \quad (38)$$

The transverse wave vectors in the medium are determined either graphically from Fig. 3 or analytically from the dispersion relation (2). The angles of refraction are given by

$$\tan \theta_{TE} = \beta / K_{TE}, \quad (39)$$

$$\tan \theta_{TM} = \beta / K_{TM}. \quad (40)$$

The angles given by (39) and (40) are the directions normal to the wave fronts of the refracted waves. The directions of energy flow are obtained by taking the normals to the normal surface.

The effect of double refraction is very pronounced near the zone boundaries where the medium is very dispersive and the band gap is different for TE and TM modes. At the edge of the band gap the group velocity which is parallel to the normal to the curve, is along the  $z$  axis and has no component normal to the interfaces. This is consistent with the fact that at or inside the gap the reflectivity is unity so that no power can flow along the  $x$  direction.

#### IV. GENERALIZED PHASE MATCHING OF NONLINEAR PROCESSES

Phase-matched enhancement of nonlinear mixing processes in a periodic stratified medium was proposed by Ashkin and Yariv,<sup>4</sup> Bloembergen and Sievers,<sup>5</sup> and recently by Tang and Bey.<sup>6</sup> Experimental evidence for this effect has been demonstrated recently by van der Ziel and Ilegems.<sup>7</sup>

In the following we present a general theory of phase matching in a periodic stratified medium. In our approach we employ the Bloch electromagnetic wave functions and their space harmonics.

Let us consider three interacting electromagnetic waves in a periodic stratified medium. The electric fields are given by their Bloch expressions

$$\mathbf{E}^{(\omega_l)}(x, z, t) = \mathbf{E}^{K_l}(x) e^{iK_l x} e^{i\beta_l z} e^{-i\omega_l t}, \quad l = 1, 2, 3, \quad (41)$$

with

$$\omega_3 = \omega_1 + \omega_2. \quad (42)$$

The  $y$  dependence is again suppressed for the sake of simplicity in illustration. Let the two media comprising the layered structure possess nonlinear optical properties which cause the two waves at  $\omega_1$  and  $\omega_2$  to generate a polarization  $\mathbf{P}(x, z)$  at  $\omega_3$  with a complex amplitude

$$P_i^{(\omega_3)}(x, z) = d_{ijk} E_j^{(\omega_1)}(x, z) E_k^{(\omega_2)}(x, z).$$

The nonlinear coupling coefficient  $d_{ijk}$ , reflecting the symmetry of the medium, is a periodic function of  $x$ ,

$$d_{ijk}^{\omega_1 + \omega_2 - \omega_3}(x + \Lambda) = d_{ijk}^{\omega_1 + \omega_2 - \omega_3}(x). \quad (43)$$

The power flowing into wave at frequency  $\omega_3$  from  $\mathbf{E}^{(\omega_1)}$  and  $\mathbf{E}^{(\omega_2)}$  is given by  $\mathbf{E}^{(\omega_3)} \cdot (\partial/\partial t) \mathbf{P}^{(\omega_3)}$ , which is proportional to

$$\langle K_3 | d | K_1 K_2 \rangle = \iint d_{ijk}(x) E_i^{K_1}(x) E_j^{K_2}(x) (E_k^{K_3}(x))^* \times e^{i(K_1 + K_2 - K_3)x} e^{i(\beta_1 + \beta_2 - \beta_3)z} dx dz, \quad (44)$$

where the superscript of  $d_{ijk}(x)$  is dropped and the integration is over the interaction region. Each of the periodic functions in the integrand may be expanded in a Fourier series

$$d_{ijk}(x) = \sum_m D_{ijk}^m e^{im(2\pi/\Lambda)x}, \quad (45)$$

$$E_i^{K_1}(x) = \sum_n A_i^n e^{in(2\pi/\Lambda)x}, \quad (46)$$

$$E_j^{K_2}(x) = \sum_l B_j^l e^{il(2\pi/\Lambda)x}, \quad (47)$$

$$E_k^{K_3}(x) = \sum_p C_k^p e^{ip(2\pi/\Lambda)x}. \quad (48)$$

Thus, we get

$$\langle K_3 | d | K_1 K_2 \rangle = (2\pi)^2 \sum_{m, n, l, p} D_{ijk}^m A_i^n B_j^l (C_k^p)^* \times \delta(K_1 + K_2 - K_3 + (m + n + l - p) \frac{2\pi}{\Lambda}) \delta(\beta_1 + \beta_2 - \beta_3). \quad (49)$$

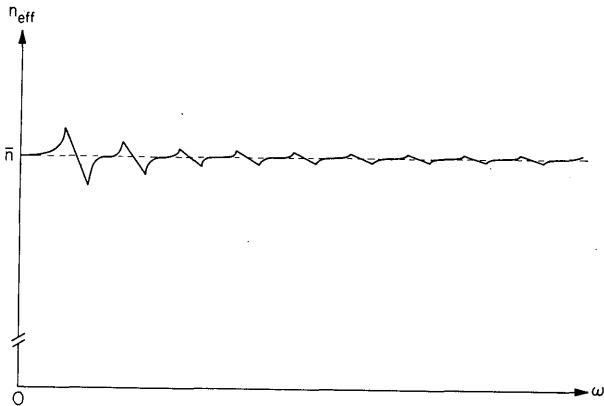


FIG. 4. Typical periodicity dispersion  $n_{\text{eff}}$  vs  $\omega$ .

We see that the nonlinear mixing is allowed only when the following two conditions are satisfied:

$$\beta_3 = \beta_1 + \beta_2, \quad (50)$$

$$K_3 = K_1 + K_2 + s(2\pi/\Lambda), \quad s = m + n + l - p. \quad (51)$$

By analogy with the corresponding phonon-phonon collisions in solid-state physics, one may classify the allowed nonlinear processes into the following two categories.

#### A. Normal nonlinear processes ( $s = 0$ )

Normal nonlinear processes in a homogeneous medium require either no dispersion or anomalous dispersion. The dispersion in a periodic stratified medium can be separated into two factors which are the natural dispersion of the material itself and the additional dispersion due to artificially periodic stratification. The latter will be called "periodicity dispersion."

A typical periodicity dispersion is shown in Fig. 4. An analytic study of the periodicity dispersion is given in Appendix B. It can be seen from Fig. 5, in which the periodicity dispersion is superposed on top of the natural dispersion, that the natural dispersion due, say, to some absorption resonance at  $\omega_0$  is modified by the periodicity dispersion. As a result, phase matching can be achieved in a spectral region where it would be impossible if the medium were homogeneous. This can be explained as follows: In order to achieve phase matching in a piecewise homogeneous medium the dispersion function  $n(\omega)$  in the relevant spectral region cannot increase monotonically. The monotony of the dispersion is removed when the periodic stratification is introduced since, as shown in Fig. 5, the change in index due to periodicity changes sign near a Bragg resonance frequency. It is therefore possible to select the parameters of the periodic structure so that phase matching is achieved in a given triplet of waves.

It is interesting to get an expression for the maximum change in the effective index of refraction which is achievable by periodicity dispersion. To be specific we derive an expression for the maximum index deviation  $\Delta n_{1/2}$  as defined in Fig. 8.

For simplicity let us consider the case of normal in-

cidence ( $\beta = 0$ ). The effective index of refraction is obtained from (10) and the relation  $v_p = c/n_{\text{eff}}$ ,

$$n_{\text{eff}}(\omega) = cK(\omega)/\omega. \quad (52)$$

Far from Bragg resonances the effective index is equal to  $\bar{n}$  where

$$\bar{n} = (n_1 a + n_2 b)/\Lambda. \quad (53)$$

The maximum deviation of  $n_{\text{eff}}$  from  $\bar{n}$  occurs at the band edges. The band edge frequencies can be approximated according to (B8b) by

$$\omega_{u,l} \cong (c/\bar{n}\Lambda) \{ (2l+1)\pi \pm 2[(\Delta-1)/(\Delta+1)]^{1/2} \}, \quad (54)$$

$$\Delta \approx 1, \quad (v/\bar{n})(l + \frac{1}{2})\pi \ll 1.$$

The maximum index deviation  $\Delta n_{1/2}$  is thus

$$\Delta n_{1/2} = n_{\text{eff}}(\omega_l) - \bar{n} = cK(\omega_l)/\omega_l - \bar{n}.$$

At the (odd) band edges ( $\omega_u, \omega_l$ ) we have

$$K(\omega_l)\Lambda = (2l+1)\pi,$$

so that

$$\Delta n_{1/2} = c(2l+1)\pi/\omega_l\Lambda - \bar{n}.$$

Substituting (54) for  $\omega_l$  in the last expression and using the fact that  $\Delta - 1 \ll 1$  leads to

$$\Delta n_{1/2} = [2\bar{n}/(2l+1)\pi] [(\Delta-1)/(\Delta+1)]^{1/2}. \quad (55)$$

From (54) we find that the width of the gap is

$$\Delta\omega_{1/2} \cong \frac{1}{2}(\omega_u - \omega_l) \approx (2c/\bar{n}\Lambda) [(\Delta-1)/(\Delta+1)]^{1/2}. \quad (56)$$

If the amount of natural dispersion that need be overcome in a given process is less than  $\Delta n_{1/2}$  given by (55), the normal nonlinear processes can achieve perfect phase matching by introducing the periodic stratification.

Phase matching can also be achieved by utilizing the birefringence property of the periodic medium. The difference in the refractive indices of the ordinary waves and extraordinary waves is given by

$$n_o - n_e = (4ab/\Lambda^2) [n_e^2/(n_o + n_e)] (\Delta^2 - 1). \quad (57)$$

However, this quantity is much smaller compared to  $\Delta n_{1/2}$  (55) for  $\Delta - 1 \ll 1$ .

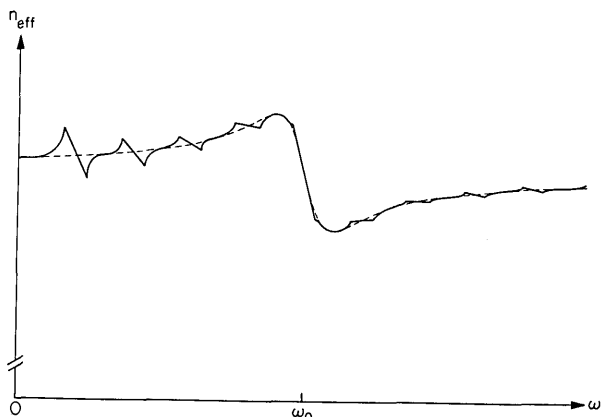


FIG. 5. Typical overall dispersion  $n_{\text{eff}}$  vs  $\omega$ .

## B. Umklapp nonlinear processes ( $s \neq 0$ )

An umklapp nonlinear process can be thought of as the generation of a wave at the mixed frequency (such as  $\omega_3 = \omega_1 + \omega_2$ ) with, simultaneously, a Bragg reflection. The additional momentum in this process is obviously provided by the periodic stratified medium (or in other words, transferred to the periodic stratified medium). Umklapp phase-matched nonlinear processes can take place in any dispersive medium under appropriate conditions. For example, the phase mismatch due to the normal dispersion of the material can always be compensated by the crystal momentum, i. e., choosing the period  $\Lambda$  so that (51) is satisfied for some combination of  $m, n, l, p$ . The missing wave momentum is thus provided by the periodicity of the integrand in (44). It can come from either the Fourier component of the nonlinear coefficient, i. e.,  $m \neq 0$  or the space harmonics of the Bloch waves, or both. The umklapp nonlinear process is thus a way to achieve phase matching when the periodicity dispersion (55) is not big enough to compensate the material dispersion.

Traditionally this process can be thought of as an interaction between the space harmonics of the Bloch waves (3) since the rate of power transfer will involve according to (49) the amplitudes of the space harmonics.

## V. DISTRIBUTED FEEDBACK SOFT-X-RAY LASERS IN PERIODIC STRATIFIED MEDIA

In this section we consider the possibility of using a layered structure as a medium for an x-ray laser. The huge pump intensities which will be required to overcome the ordinary photoelectric losses in the x-ray region will limit the pumped region to very small volumes. Under these conditions the use of an external resonator structure seems highly unlikely. One proposal advanced earlier<sup>6</sup> was to use the periodicity of natural crystal to provide distributed feedback by Bragg reflection. In what follows we consider the possibility of obtaining Bragg x-ray laser action in artificial layered media. In such media we have the freedom of tailoring the period exactly so that the Bragg condition is satisfied at the oscillation wavelength. In addition no crystals exist in which the unit cell dimensions are comparable to oscillation wavelengths of, say, 100 Å.

We will thus consider a layered medium in which one of the layers provides gain at some frequency  $\omega$ . Since the presence of gain or loss can be represented by the use of complex indices of refraction we need to extend the analysis of paper I to the case of media with complex indices. The coefficient of reflectivity of the  $N$  layered structure is given as in (33) of paper I by

$$r_N = C U_{N-1} / (A U_{N-1} - U_{N-2}), \quad (58)$$

while the transmission is

$$t_N = (A U_{N-1} - U_{N-2})^{-1}. \quad (59)$$

The complex indices of refraction are taken as

$$\hat{n}_1 = n_1 + i\kappa_1, \quad (60)$$

$$\hat{n}_2 = n_2 + i\kappa_2. \quad (61)$$

The imaginary part of a refractive index is directly related to the bulk loss constant (or gain) by the following relation:

$$\alpha_{1,2} = 2\kappa_{1,2}\omega/c. \quad (62)$$

Consider next a periodic stratified medium with alternating gain and loss layers ( $\alpha_1 > 0$ ,  $\alpha_2 < 0$ ).

Such a structure could result if we were to fabricate, as an example, an artificial layered medium composed alternately of two media—1 and 2—and then pump it by an incoherent x-ray beam or an intense laser source. Since the layers are different the effect of the pump can be to produce an inversion in layers 2, say, at some characteristic x-ray frequency. We thus have a situation where x-ray radiation of the characteristic frequency is amplified in layers 2 but is absorbed by the photoelectric effect in layers 1. We will show next that if the unit cell (i. e., the alternation period) length  $\Lambda$  is chosen near the Bragg value  $\frac{1}{2}l\lambda_g$  then oscillation may result. The determination of the pump threshold requires an exact formulation of the electromagnetic problem. This becomes possible with the aid of the Bloch formalism developed in paper I.

We choose  $n_1$  and  $n_2$  as well as  $\alpha_1$  as parameters, take the layer thicknesses  $a = b = \frac{1}{2}\Lambda$ , and investigate the reflectivity  $r_N$  of a ten-period slab ( $N = 10$ ) as a function of  $\omega\Lambda/c$  and  $\alpha_2$ . The contour plot of  $|r_N|$  in the  $\alpha_2$ - $\omega$  plane are shown in Fig. 6. A series of points where  $|r_N| = \infty$  is found in the lower half-plane ( $\alpha_2 < 0$ ). The coordinates of these poles correspond to the threshold gains and the oscillation frequencies of the laser. The number of poles is exactly  $N$ , which is the number of periods. The pole trajectory in the  $\alpha_2$ - $\omega$  plane indicates that the pole nearest the bandgap has the lowest threshold gain. The threshold gain  $\alpha_{2t}$  is approximately equal to loss  $\alpha_1$  for modes whose frequency is far away from the band gap. However, it is much less than the loss when the oscillation is near the band gap. In our example,  $|\alpha_{2t}| \approx \frac{1}{3}\alpha_1$ . This theoretical result can be explained as follows: The power dissipation per unit area is proportional to

$$J = \int \alpha(x) E^2(x) dx, \quad (63)$$

where

$$\alpha(x) = \begin{cases} \alpha_1 > 0, & \text{layer 1,} \\ \alpha_2 < 0, & \text{layer 2.} \end{cases} \quad (64)$$

If the lasing mode intensity distribution can have its maxima in the gain layers and minima in the loss layers, power generation ( $J < 0$ ) is possible even when the integrated loss is positive, or in other words when

$$\int \alpha(x) dx > 0. \quad (65)$$

In the conventional Fabry-Perot laser where  $\alpha(x) = \text{constant}$ , power generation requires a net positive gain (negative loss)

$$\alpha L < 0. \quad (66)$$

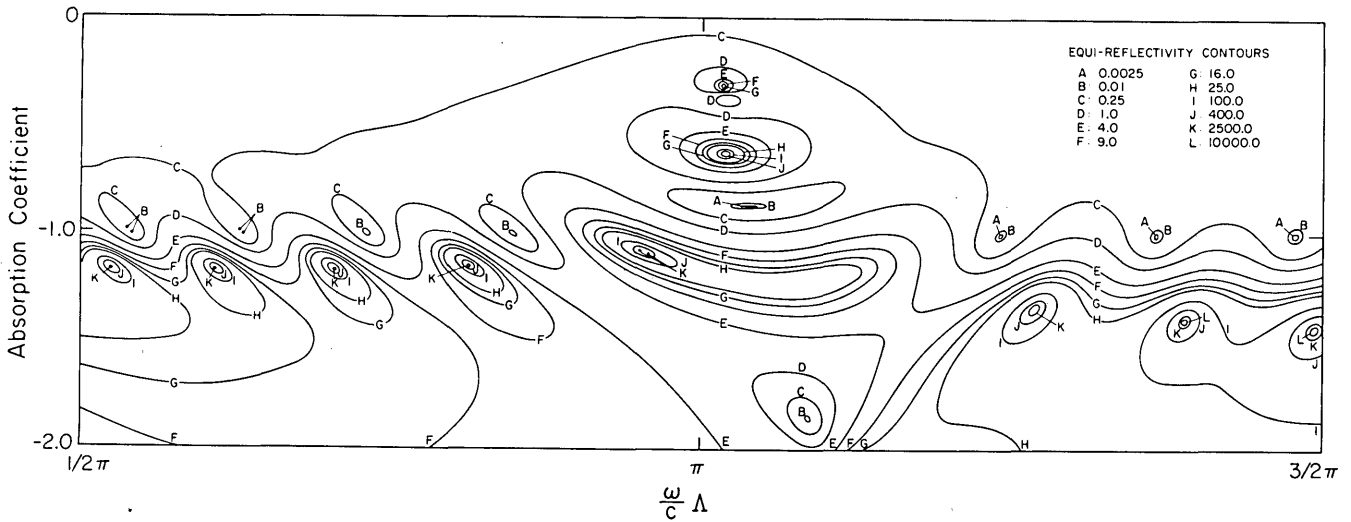


FIG. 6. Contours of equal reflectivity in  $\omega-\alpha_2$  plane.

That means the laser medium of the conventional laser has to be pumped until the gain conquers the loss. However, in a periodic multilayer laser the gain constant of the gain layer does not have to be larger than the loss constant of the loss layer assuming the same layer thickness. This is similar to the "Borrmann effect" of an x-ray propagating in a crystal.<sup>9</sup> This finding is of important significance to x-ray lasers since it should make possible significant reductions in the threshold pumping requirements.

The field distribution near oscillation of a typical multilayer x-ray laser is shown in Fig. 7. Note that the local maxima of the field amplitude are all located in the gain layers. The parameters correspond to the low threshold pole of Fig. 6.

## VI. CONCLUSION

The matrix Bloch wave formalism has been used to derive the dispersion behavior of electromagnetic modes in layered periodic media. The use of periodic media in phase matching nonlinear optical interactions was considered as well as their use in obtaining reduced threshold x-ray lasers.

## APPENDIX A: VELOCITY OF ENERGY FLOW AND GROUP VELOCITY

The time-averaged flux of energy in an electromagnetic field is given by

$$\mathbf{S} = \frac{1}{2} \text{Re}[\mathbf{E} \times \mathbf{H}^*]. \quad (\text{A1})$$

The time-averaged electromagnetic energy density is given by

$$U = \frac{1}{4} (\epsilon |\mathbf{E}|^2 + \mu |\mathbf{H}|^2). \quad (\text{A2})$$

In the case of a propagating Bloch wave in a periodic structure,  $\mathbf{S}$  and  $U$  are both periodic functions of  $x$  with a period  $\Lambda$ . It is desirable to define the space-averaged quantities in a periodic medium. The mean values over one period for  $U$  and  $\mathbf{S}$  are given by

$$\langle U \rangle = \frac{1}{\Lambda} \int_0^\Lambda U(x) dx, \quad (\text{A3})$$

$$\langle \mathbf{S} \rangle = \frac{1}{\Lambda} \int_0^\Lambda \mathbf{S}(x) dx. \quad (\text{A4})$$

The velocity of energy flow is defined

$$\mathbf{V}_e = \langle \mathbf{S} \rangle / \langle U \rangle, \quad (\text{A5})$$

which gives the rate at which energy flows from one cell to the next in a periodic medium. The group velocity of a wave propagating in the same medium may be taken as

$$\mathbf{V}_g = \left( \frac{\partial \omega}{\partial K} \right)_\beta \hat{a}_x + \left( \frac{\partial \omega}{\partial \beta} \right)_K \hat{a}_z. \quad (\text{A6})$$

It is the purpose of this appendix to prove that

$$\mathbf{V}_g = \mathbf{V}_e. \quad (\text{A7})$$

Equation (A7) will be proved in the case of TE Bloch waves. The electric field distribution for a TE Bloch wave is given by (5):

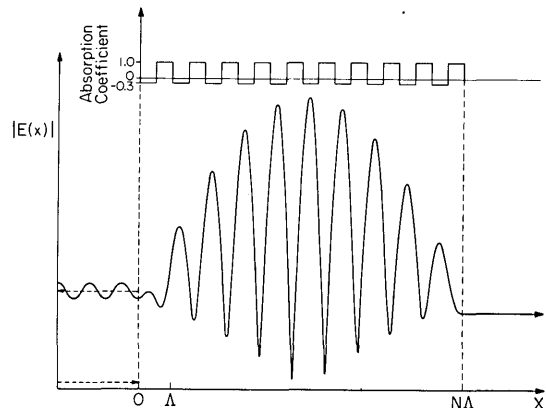


FIG. 7. Field distribution near oscillation. The dashed arrows indicate incident and reflected waves, respectively. The solid arrow at the right-hand side indicates the transmitted wave. The inset in the upper part is the gain-loss profile.

$$E_y(x, z) = E_K(x) e^{iKx} e^{i\beta z} \quad (\text{A8})$$

$$= \begin{cases} (a_0 e^{ik_{1x}x} + b_0 e^{-ik_{1x}x}) e^{i\beta z} e^{-i\omega t}, & -a < x < 0, \\ (c_0 e^{ik_{2x}x} + d_0 e^{-ik_{2x}x}) e^{i\beta z} e^{-i\omega t}, & -\Lambda < x < -a. \end{cases} \quad (\text{A9})$$

The corresponding magnetic field is given by

$$H_x(x, z) = -(\beta/\omega\mu)E_y(x, z), \quad (\text{A10})$$

$$H_z(x, z) = \begin{cases} (k_{1x}/\omega\mu)(a_0 e^{ik_{1x}x} - b_0 e^{-ik_{1x}x}) \times e^{i\beta z}, & -a < x < 0, \\ (k_{2x}/\omega\mu)(c_0 e^{ik_{2x}x} - d_0 e^{-ik_{2x}x}) \times e^{i\beta z}, & -\Lambda < x < -a, \end{cases} \quad (\text{A11})$$

where

$$\begin{pmatrix} a_0 \\ b_0 \end{pmatrix} = \begin{pmatrix} B \\ e^{-iK\Lambda} - A \end{pmatrix}, \quad (\text{A12})$$

$$\begin{pmatrix} c_0 e^{-ik_{2x}a} \\ d_0 e^{ik_{2x}a} \end{pmatrix} = \begin{pmatrix} \frac{1}{2}(1 + k_{1x}/k_{2x}) & \frac{1}{2}(1 - k_{1x}/k_{2x}) \\ \frac{1}{2}(1 - k_{1x}/k_{2x}) & \frac{1}{2}(1 + k_{1x}/k_{2x}) \end{pmatrix} \times \begin{pmatrix} a_0 e^{-ik_{1x}a} \\ b_0 e^{ik_{1x}a} \end{pmatrix}. \quad (\text{A13})$$

From (A2), (A3), (A9), (A10), and (A11) the averaged energy density is calculated to be

$$\langle U \rangle = \frac{1}{2} \left[ \frac{a}{\Lambda} \epsilon_1 (|a_0|^2 + |b_0|^2) + \frac{b}{\Lambda} \epsilon_2 (|c_0|^2 + |d_0|^2) + \frac{B+C}{\Lambda} \cdot \frac{\beta^2}{\omega^2 \mu} k_{1x} \left( \frac{1}{k_{1x}^2} - \frac{1}{k_{2x}^2} \right) \left( \sin K\Lambda - i \frac{A-D}{2} \right) \right]. \quad (\text{A14})$$

From (A1), (A4), (A9), (A10), and (A11) the averaged Poynting vector is given by

$$\langle S_x \rangle = S_x = \frac{1}{2} \frac{k_{1x}}{\omega\mu} (|a_0|^2 - |b_0|^2) = \frac{1}{2} \frac{k_{2x}}{\omega\mu} (|c_0|^2 - |d_0|^2), \quad (\text{A15})$$

$$\langle S_z \rangle = \frac{1}{2} \frac{\beta}{\omega\mu} \left[ \frac{a}{\Lambda} (|a_0|^2 + |b_0|^2) + \frac{b}{\Lambda} (|c_0|^2 + |d_0|^2) + \frac{B+C}{\Lambda} \cdot k_{1x} \left( \frac{1}{k_{1x}^2} - \frac{1}{k_{2x}^2} \right) \left( \sin K\Lambda - i \frac{A-D}{2} \right) \right]. \quad (\text{A16})$$

The group velocity can be obtained by using implicit differentiation. Given a function  $F(\omega, \beta, K) = 0$ , we can write (A6) as

$$\mathbf{V}_g = - \left[ \left( \frac{\partial F}{\partial K} \right)_{\omega, \beta} / \left( \frac{\partial F}{\partial \omega} \right)_{K, \beta} \right] \hat{a}_x - \left[ \left( \frac{\partial F}{\partial \beta} \right)_{\omega, K} / \left( \frac{\partial F}{\partial \omega} \right)_{K, \beta} \right] \hat{a}_z, \quad (\text{A17})$$

where, using (2),

$$F(\omega, \beta, K) = \cos K\Lambda - \frac{1}{2}(A+D). \quad (\text{A18})$$

From (A17) and (A18),  $V_{gx}$  and  $V_{gz}$  are obtained as

$$V_{gx} = \Lambda \sin K\Lambda \left/ \left[ i \left( \frac{A-D}{2} \right) \frac{an_1^2 \omega}{k_{1x} c^2} + i \left( \frac{\bar{A}-\bar{D}}{2} \right) \frac{bn_2^2 \omega}{k_{2x} c^2} - \frac{B+C}{2} \left( \frac{n_1^2 \omega}{k_{1x} c^2} - \frac{n_2^2 \omega}{k_{2x} c^2} \right) \right] \right., \quad (\text{A19})$$

$$V_{gz} = \left[ i \left( \frac{A-D}{2} \right) \frac{a\beta}{k_{1x}} + i \left( \frac{\bar{A}-\bar{D}}{2} \right) \frac{b\beta}{k_{2x}} - \frac{B+C}{2} \beta \left( \frac{1}{k_{1x}^2} - \frac{1}{k_{2x}^2} \right) \right] \times \left[ i \left( \frac{A-D}{2} \right) \frac{an_1^2 \omega}{k_{1x} c^2} + i \left( \frac{\bar{A}-\bar{D}}{2} \right) \frac{bn_2^2 \omega}{k_{2x} c^2} - \frac{B+C}{2} \left( \frac{n_1^2 \omega}{k_{1x} c^2} - \frac{n_2^2 \omega}{k_{2x} c^2} \right) \right]^{-1}, \quad (\text{A20})$$

where

$$\bar{A} = e^{-ik_{2x}b} \left[ \cos k_{1x}a - \frac{1}{2}i \left( \frac{k_{2x}}{k_{1x}} + \frac{k_{1x}}{k_{2x}} \right) \sin k_{1x}a \right], \quad (\text{A21})$$

$$\bar{D} = e^{ik_{2x}b} \left[ \cos k_{1x}a + \frac{1}{2}i \left( \frac{k_{2x}}{k_{1x}} + \frac{k_{1x}}{k_{2x}} \right) \sin k_{1x}a \right]. \quad (\text{A22})$$

It follows from (A5), (A14), (A15), and (A16) that the velocity of energy flow is given by

$$V_{ex} = \left[ \frac{a}{\Lambda} \frac{\omega\mu\epsilon_1}{k_{1x}} \frac{|a_0|^2 + |b_0|^2}{|a_0|^2 - |b_0|^2} + \frac{b}{\Lambda} \frac{\omega\mu\epsilon_2}{k_{2x}} \frac{|c_0|^2 + |d_0|^2}{|c_0|^2 - |d_0|^2} + \frac{B+C}{\Lambda} \frac{\beta^2}{\omega} \left( \frac{1}{k_{1x}^2} - \frac{1}{k_{2x}^2} \right) \frac{\sin K\Lambda - i(A-D)/2}{|a_0|^2 - |b_0|^2} \right]^{-1}, \quad (\text{A23})$$

$$V_{ez} = \frac{\beta}{\omega\mu} \left[ \frac{a}{\Lambda} (|a_0|^2 + |b_0|^2) + \frac{b}{\Lambda} (|c_0|^2 + |d_0|^2) + \frac{B+C}{\Lambda} k_{1x} \left( \frac{1}{k_{1x}^2} - \frac{1}{k_{2x}^2} \right) \left( \sin K\Lambda - i \frac{A-D}{2} \right) \right] \times \left[ \frac{a\epsilon_1}{\Lambda} (|a_0|^2 + |b_0|^2) + \frac{b\epsilon_2}{\Lambda} (|c_0|^2 + |d_0|^2) + \frac{B+C}{\Lambda} \cdot \frac{\beta^2}{\omega^2 \mu} k_{1x} \left( \frac{1}{k_{1x}^2} - \frac{1}{k_{2x}^2} \right) \left( \sin K\Lambda - i \frac{A-D}{2} \right) \right]^{-1}. \quad (\text{A24})$$

If we introduce the following three parameters

$$X \equiv (|a_0|^2 + |b_0|^2) / (|a_0|^2 - |b_0|^2), \quad (\text{A25})$$

$$Y \equiv (|c_0|^2 + |d_0|^2) / (|c_0|^2 - |d_0|^2), \quad (\text{A26})$$

$$Z \equiv [\sin K\Lambda - i(A-D)/2] / (|a_0|^2 - |b_0|^2), \quad (\text{A27})$$

the velocity of energy flow (A23) and (A24) can be written

$$V_{ex} = \left[ \frac{a}{\Lambda} \cdot \frac{\omega\mu\epsilon_1}{k_{1x}} X + \frac{b}{\Lambda} \frac{\omega\mu\epsilon_2}{k_{2x}} Y + \frac{B+C}{\Lambda} \cdot \frac{\beta^2}{\omega} \left( \frac{1}{k_{1x}^2} - \frac{1}{k_{2x}^2} \right) Z \right]^{-1}, \quad (\text{A28})$$

$$V_{ez} = \left[ \frac{a}{\Lambda} \cdot \frac{\beta}{k_{1x}} X + \frac{b}{\Lambda} \cdot \frac{\beta}{k_{2x}} Y + \frac{B+C}{\Lambda} \left( \frac{1}{k_{1x}^2} - \frac{1}{k_{2x}^2} \right) Z \right] \times \left[ \frac{a}{\Lambda} \cdot \frac{\omega\mu\epsilon_1}{k_{1x}} X + \frac{b}{\Lambda} \cdot \frac{\omega\mu\epsilon_2}{k_{2x}} Y + \frac{B+C}{\Lambda} \cdot \frac{\beta^2}{\omega} \left( \frac{1}{k_{1x}^2} - \frac{1}{k_{2x}^2} \right) Z \right]^{-1}. \quad (\text{A29})$$

The last equality relation of (A15) was used to derive the above two equations.

It can be shown from (A12), (A13), (A25), (A26), and (A27) that

$$X = \frac{i[(A-D)/2]}{\sin K\Lambda}, \quad (\text{A30})$$

$$Y = \frac{i[(\bar{A}-\bar{D})/2]}{\sin K\Lambda}, \quad (\text{A31})$$

$$Z = -(2 \sin K\Lambda)^{-1}. \quad (\text{A32})$$

This proves our statement (A7).

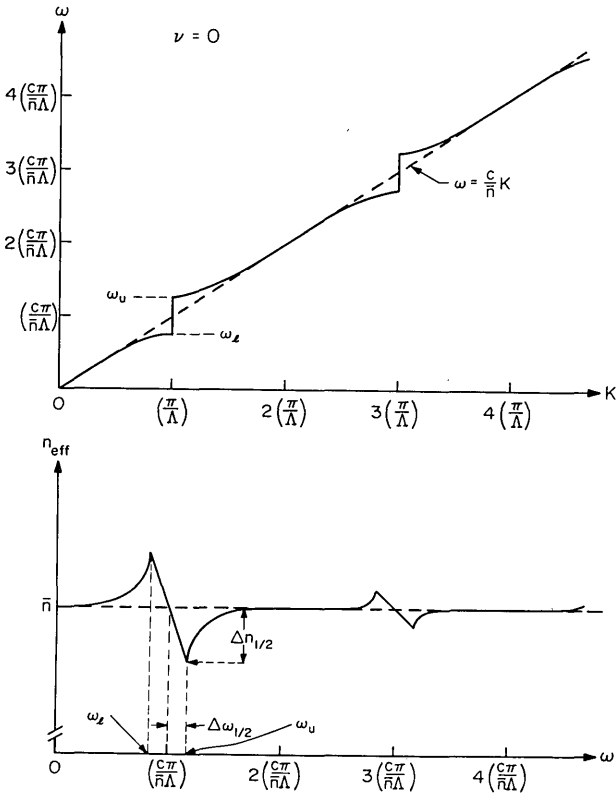


FIG. 8. Periodicity dispersion when  $n_1a = n_2b$  (or  $\nu = 0$ ).

## APPENDIX B: PERIODICITY DISPERSION OF STRATIFIED MEDIA

In this appendix we treat analytically and quantitatively the periodicity dispersion. We obtain expressions for the locations and sizes of the band gaps. We will limit our derivation to the case of normal incidence. The extension of our result to the general case will be given in the last part of this appendix.

Instead of using  $n_1$ ,  $n_2$ ,  $a$ , and  $b$ , a new set of more convenient parameters will be defined in the following:

$$\Delta = \frac{1}{2}(n_2/n_1 + n_1/n_2), \quad (\text{B1})$$

$$\bar{n} = (n_1a + n_2b)/\Lambda, \quad (\text{B2})$$

$$\nu = (n_1a - n_2b)/\Lambda. \quad (\text{B3})$$

In terms of these new parameters, the dispersion relation (2) can be written

$$\cos K\Lambda = \left(\frac{\Delta+1}{2}\right) \cos \bar{n} \frac{\omega}{c} \Lambda - \left(\frac{\Delta-1}{2}\right) \cos \nu \frac{\omega}{c} \Lambda. \quad (\text{B4})$$

By using the following identity

$$\cos x = 1 - 2 \sin^2 x/2, \quad (\text{B5})$$

Eq. (B4) can be written

$$\sin^2 \frac{K\Lambda}{2} = \left(\frac{\Delta+1}{2}\right) \sin^2 \frac{\bar{n}\omega}{2c} \Lambda - \left(\frac{\Delta-1}{2}\right) \sin^2 \frac{\nu\omega}{2c} \Lambda. \quad (\text{B6})$$

This equation is especially useful when  $\nu \ll \bar{n}$ . In the event when  $\nu = 0$  ( $n_1a = n_2b$ ), Eq. (B6) gives us the explicit form of  $\omega$  as a function of  $K$ .

The locations of band edges can be obtained from

(B6). If we set  $K\Lambda = m\pi$ , we obtain

$$\sin^2 \left( \frac{\bar{n}\omega}{2c} \Lambda \right) = \begin{cases} \left( \frac{\Delta-1}{\Delta+1} \right) \sin^2 \left( \frac{\nu\omega}{2c} \Lambda \right), & K\Lambda = 2l\pi, \\ 1 - \left( \frac{\Delta-1}{\Delta+1} \right) \cos^2 \left( \frac{\nu\omega}{2c} \Lambda \right), & K\Lambda = (2l+1)\pi, \end{cases} \quad (\text{B7})$$

where  $l$  is an integer. If  $\nu \ll \bar{n}$  which is normally true, Eq. (B7) can be solved by the method of successive approximation. The results for the upper and lower band edge frequencies after one iteration are given by

$$\omega_{u,l} \approx \begin{cases} \frac{c}{\bar{n}\Lambda} \left\{ 2l\pi + 2 \sin^{-1} \left[ \left( \frac{\Delta-1}{\Delta+1} \right)^{1/2} \sin \left( \frac{\nu}{\bar{n}} l\pi \right) \right] \right\}, & K\Lambda = 2l\pi, \\ \frac{c}{\bar{n}\Lambda} \left\{ (2l+1)\pi + 2 \sin^{-1} \left[ \left( \frac{\Delta-1}{\Delta+1} \right)^{1/2} \cos \left( \frac{\nu}{\bar{n}} \left( l + \frac{1}{2} \right) \pi \right) \right] \right\}, & K\Lambda = (2l+1)\pi. \end{cases} \quad (\text{B8a})$$

$$K\Lambda = (2l+1)\pi. \quad (\text{B8b})$$

Consider a stratified medium consisting of alternating layers of the same optical thickness which is the case when  $\nu = 0$ , all the even-order band gaps shrink to zero, while the odd-order band gaps have a maximum constant value

$$\Delta\omega_{\max} = \frac{4c}{\bar{n}\Lambda} \sin^{-1} \left( \frac{\Delta-1}{\Delta+1} \right)^{1/2}, \quad (\text{B9})$$

and the centers of the band gaps are all on the same straight line

$$\omega = (c/\bar{n})K. \quad (\text{B10})$$

The vanishing of the even-order band gaps is due to the fact that each layer becomes a half-wave layer at the even-order Bragg conditions so that reflections from two adjacent interfaces are out of phase by an odd multiple of it. The dispersion relation for this special case is shown in Fig. 8.

In the general case when  $\nu \neq 0$ , the degeneracy is removed and there is, in general, a finite band gap at  $K\Lambda = 2l\pi$ . The band edges of each forbidden gap are always on both sides of the straight line  $\omega = cK/\bar{n}$ . The band gap sizes vary roughly periodically as a function of the Bragg order for even orders and odd orders separately. This can be seen from either (B8) or Fig. 9, which is a plot of both sides of (B7) and gives a graph-

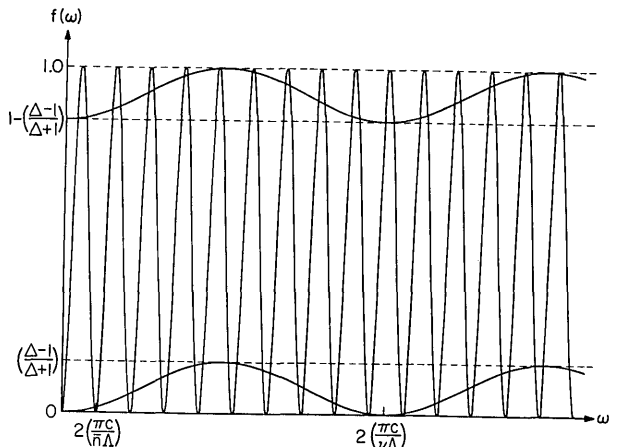


FIG. 9. Graphic method of finding band edges and gap sizes.

ic solution of the locations of band edges. The band gaps are given approximately by

$$\Delta\omega_{\text{gap}} = \begin{cases} \frac{4c}{\bar{n}\Lambda} \sin^{-1} \left( \frac{\Delta-1}{\Delta+1} \right)^{1/2} \sin \left( \frac{\nu}{\bar{n}} l\pi \right), & K\Lambda = 2l\pi, \\ \frac{4c}{\bar{n}\Lambda} \sin^{-1} \left( \frac{\Delta-1}{\Delta+1} \right)^{1/2} \cos \left( \frac{\nu}{\bar{n}} \left( l + \frac{1}{2} \right) \pi \right), & K\Lambda = (2l+1)\pi. \end{cases} \quad (\text{B11})$$

In the usual case of inclined incidence ( $\beta \neq 0$ ), all the above results are applicable provided  $\Delta$ ,  $\bar{n}$ , and  $\nu$  are defined by

$$\Delta = \begin{cases} \frac{1}{2} \left( \frac{n_2 \cos \theta_2}{n_1 \cos \theta_1} + \frac{n_1 \cos \theta_1}{n_2 \cos \theta_2} \right), & \text{TE waves,} \\ \frac{1}{2} \left( \frac{n_1 \cos \theta_2}{n_2 \cos \theta_1} + \frac{n_2 \cos \theta_1}{n_1 \cos \theta_2} \right), & \text{TM waves,} \end{cases} \quad (\text{B12})$$

$$\bar{n} = (n_1 a \cos \theta_1 + n_2 b \cos \theta_2) / \Lambda, \quad (\text{B13})$$

$$\nu = (n_1 a \cos \theta_1 - n_2 b \cos \theta_2) / \Lambda, \quad (\text{B14})$$

where

$$\cos \theta_1 = ck_{1x} / n_1 \omega, \quad (\text{B15})$$

$$\cos \theta_2 = ck_{2x} / n_2 \omega. \quad (\text{B16})$$

It can be seen from (B8) that the locations of the band gaps are shifted toward higher frequencies and the sizes of the band gaps become larger at inclined incidence.

\*Research supported by the Office of Naval Research and the NSF.

<sup>1</sup>P. Yeh, A. Yariv, and C. S. Hong, "Electromagnetic propagation in periodic stratified media. I. General theory," *J. Opt. Soc. Am.* 67, 423-438 (1977) (preceding paper).

<sup>2</sup>See, for example, A. Yariv, *Quantum Electronics*, 2nd. ed. (Wiley, New York, 1975), p. 85.

<sup>3</sup>S. M. Rytov, *Sov. Phys. -JETP* 2, 446 (1956).

<sup>4</sup>A. Ashkin and A. Yariv, Bell Labs. Tech. Memo No. MM-61-124-46 (13 November 1961) (unpublished).

<sup>5</sup>N. Bloembergen and A. J. Sievers, *Appl. Phys. Lett.* 17, 483 (1970).

<sup>6</sup>C. L. Tang and P. P. Bey, *IEEE J. Quant. Electron.* QE-9, 9 (1973).

<sup>7</sup>J. P. van der Ziel and M. Ilegems, *Appl. Phys. Lett.* 28, 437 (1976).

<sup>8</sup>A. Yariv, *Appl. Phys. Lett.* 25, 105 (1974).

<sup>9</sup>B. W. Batterman, *Rev. Mod. Phys.* 36, 681 (1964).

## Interference theory of reflection from multilayered media

Neil Ashby and Stanley C. Miller

*Department of Physics and Astrophysics, University of Colorado, Boulder, Colorado 80309*

(Received 25 September 1976; revision received 15 December 1976)

Interference effects normal to the plane of incidence are calculated for a light beam incident on a reflecting surface consisting of several parallel thin layers. Resonances that arise when one of the thin layers acts as a two-dimensional waveguide give rise to phase shifts of the plane waves in the reflected beam which vary rapidly with the angle of incidence. Interference in the reflected beam can then sometimes give it the appearance of a diffraction pattern. The results are compared with Levy and Imbert's recent experiment.

### I. INTRODUCTION

When plane light waves undergo total internal reflection from a plane interface between dielectric media, the reflected waves are shifted in phase as a result of the interactions between the light and the reflecting media. These phase shifts can give rise to interesting interference effects causing changes in position and shape of wave packets constructed out of plane waves. Longitudinal shifts in position (in the plane of incidence), arising from reflection at a single (nonlayered) surface were first predicted and observed by Goos and Hänchen.<sup>1</sup> Experimental observations of this effect have been carried out primarily by Imbert and coworkers<sup>2,3</sup> in recent years. Lotsch<sup>4</sup> has given an extensive review of the Goos-Hänchen shifts.

Similarly, transverse shifts in position (normal to the incidence plane) occur at critical reflection. This was first predicted by Federov.<sup>5</sup> The phenomenon has been studied experimentally by Imbert,<sup>6</sup> and de Beaugard and Imbert.<sup>3</sup>

There have been several different approaches to the

theoretical description of these phenomena. De Beaugard,<sup>7</sup> Imbert,<sup>6,8</sup> and Ricard<sup>9</sup> have discussed the transverse shifts on the basis of transverse Poynting vector energy flows in the evanescent waves. Expressions for the transverse shifts based on the method of stationary phase have been obtained by Schilling,<sup>10</sup> Boulware,<sup>11</sup> and Ashby and Miller<sup>12</sup>; these expressions do not agree well with the predictions based on a Poynting vector.

Ashby and Miller<sup>12</sup> have approached the calculation of the transverse shift and shape by constructing wave packets which are modified by phase factors arising from the internal reflection process. This approach appears to be the only feasible one in cases where the stationary phase method gives divergent results (at the critical angle), or when the primary effects are changes in the shape of the packet due to interference.

Similar effects have been observed in layered structures. Here one or more thin layers, which act like a two-dimensional waveguide, are partially isolated from the first reflecting surface. Due to resonances which